Thermochimica Acta 512 (2011) 189–195

Contents lists available at ScienceDirect

Thermochimica Acta

journal homepage: www.elsevier.com/locate/tca

Thermodynamics of the Al_3Ni phase and revision of the Al–Ni system

H.-L. Chen[a,*], E. Doernberg[a], P. Svoboda[b], R. Schmid-Fetzer[a]

[a] Institute of Metallurgy, Clausthal University of Technology, Robert-Koch-Straße 42, D-38678 Clausthal-Zellerfeld, Germany
[b] Department of Electronic Structures, Faculty of Mathematics and Physics, Charles University, Ke Karlovu 5, 120 00 Prague 2, Czech Republic

ARTICLE INFO

Article history:
Received 22 August 2010
Received in revised form 1 October 2010
Accepted 11 October 2010
Available online 19 October 2010

Keywords:
Drop calorimeter
Relaxation method
Heat capacity
Thermodynamics

ABSTRACT

The heat capacity of the Al_3Ni phase had been measured for the first time, by means of relaxation method over the low temperature range 2–323 K and by measuring heat content increments using drop calorimetry over the higher temperature range of 583–1073 K. The Debye function was employed to fit the low-temperature heat capacities, and from the function, the absolute entropy was evaluated, $S^{\circ}_{298} = 25.4$ J/mol-atoms K. A three-term polynomial representation, $a+b{\cdot}T+c{\cdot}T^{-2}$, was used for describing heat capacity above 298.15 K. The Gibbs energy function of the Al_3Ni phase was derived with a fixed reference state by incorporating the polynomial expression of the heat capacity, the recently reported enthalpy of formation and the related phase equilibria in the Al–Ni system. A revised thermodynamic description of the entire Al–Ni system together with the calculated phase diagram is also presented.

1. Introduction

The phase diagram of the Al–Ni system is rather well established and even thermodynamic modeling has been conducted by a number of investigators [1–4]. The early work of Ansara et al. [2] gave a first attempt to describe order–disorder transition. Following that work and using the Al–Ni system as the example, Ansara and Dupin [5–7] put great efforts in the modeling of the order–disorder transition between fcc_A1 and $L1_2$ and that between bcc_A2 and B2. As a result, the thermodynamic description of the Al–Ni system had been updated several times. The latest description due to Dupin et al. [7] reproduces both the phase equilibrium data and thermodynamic properties of the Al–Ni system well. However, some aspects concerning the B2 phase and Al-rich phases prompted a revision as detailed below.

A recent work conducted by some of the current authors [8] presented a method that uses compound energy formalism to describe the vacancy properties by reviewing (Va):(Va) as being a solution member rather than as being a compound end member. As a demonstration, the B2 phase in the Al–Ni system was remodeled due to its high vacancy concentration, with the descriptions for other phases accepted from Dupin et al. [7].

Motivated by the investigation of the peritectic solidification in Al-rich Al–Ni alloys, which is conducted by coupling phase-field simulation with directional solidification experiments [9], the present work is to provide a much more accurate Gibbs energy description of the Al-rich phases as input for a precise phase-field modeling. Heat capacity is considered to be a key property of a phase. If determined over the full temperature range it allows for an independent determination of the absolute entropy of the phase in addition to a more precise Gibbs energy function compared to the current Neumann–Kopp-rule approximation. This allows the thermodynamic properties to be manipulated with confidence. In this work, the heat capacity of the Al_3Ni phase will be measured for the first time, and its Gibbs energy description be derived by taking into accounting the expression of heat capacity, and incorporating the reported enthalpy of formation and the related phase equilibria. Due to the new descriptions of B2 [8] and Al_3Ni, the descriptions of liquid and Al_3Ni_2 will be adjusted compared to the basic work by Dupin et al. [7], in order to provide a better agreement with the phase equilibria in that composition region.

2. Experiments

2.1. Sample preparation for heat capacity measurements

Commercial Al_3Ni powders[1] (<150 μm, Goodfellow Cambridge Ltd.) were compressed into cylindrical pellets under a 10 KN compressing force. Previous X-ray powder diffraction (XRD) exam-

[1] The powders had been prepared at an Al/Ni ratio of 3/1. XRD showed that the Al_3Ni_2 and (Al) phases exist and the materials had not been fully transformed to the Al_3Ni phase. The purity was not given in the product identification, while our chemical analysis of the powders detected 0.37 wt.% aluminum oxide. After being annealed at 800 °C for 4 days, only the Al_3Ni phase was identified by XRD and BSE and SEI examination.

* Corresponding author. Tel.: +49 05323 72 2077; fax: +49 05323 72 3120.
E-mail address: CompMS@163.com (H.-L. Chen).

0040-6031/$ – see front matter © 2010 Elsevier B.V. All rights reserved.
doi:10.1016/j.tca.2010.10.005

inations showed that the as-purchased powders are not of Al_3Ni-single phase but contain traces of Al and Al_3Ni_2. The pellets were contained in Al_2O_3 crucibles (that had been manufactured for DTA), separately encapsulated in evacuated quartz tubes (10^{-2} mbar), and then annealed at 800 °C for 4 days followed by cooling in the furnace.

After being annealed, randomly selected samples were subjected to phase identifications by XRD using a Siemens D5000 diffractometer (Siemens, Germany). The XRD examination was conducted using Co-Kα radiation in the range of $20° < 2\theta < 90°$ with a step size of 0.005° every 2 s. A supplementary examination of the backscattered electron images (BSE) and the secondary electron images (SEI) was also performed on the well-polished samples under scanning electron microscopy. These samples were confirmed to be in the single-phase state.

2.2. Relaxation method

The PPMS equipment 14 T-type (Quantum Design, USA) was used for heat capacity measurements of Al_3Ni in the low-temperature region. The two samples for the PPMS apparatus were plates of 10.41 mg and 10.86 mg. The sample was mounted to the calorimeter platform with Apiezon N grease (supplied by Quantum Design). A sample holder with the Apiezon only was measured in the temperature range 2–323 K to obtain background data, then the sample plate was attached to the calorimeter with Apiezon and the measurement was repeated in the same temperature range with the same temperature steps. The sample specific heat was then obtained as the difference of the two data sets. The heat capacity measurements in the PPMS were performed by the relaxation method with fully automatic procedure under high vacuum ($\sim 10^{-2}$ Pa) to avoid heat loss through the exchange gas. The relative accuracy of the heat capacity data was estimated to be better than 2% [10].

2.3. Drop calorimetry

In order to determine the high-temperature heat capacities of the Al_3Ni phase, the heat contents were measured using a drop Calorimeter (MHTC Line 96, multi detector, Setaram, France) over the temperature range 573–1073 K. The working cell was under a flowing helium atmosphere. At each temperature, five samples and six references (sapphire, NIST SRM no. 720) were dropped alternately from room temperature into an alumina crucible (13 mm in diameter, 40 mm in height) kept at the selected high temperature. The time interval between each successive two drops is between 25 and 30 min. The alumina crucible was filled with alumina powders (γ-Al_2O_3, 70% particles having sizes of 0.063–0.2 mm) up to one third height so that the sample will fall into the detector's most sensitive area. The weight of each sample was around 100 mg and the sapphire around 90 mg. Each drop of sapphire helps to determine the sensitivity of the drop calorimeter. Prior to and after each drop of the Al_3Ni sample, the two drops of sapphires could provide an averaged sensitivity for determining the heat content increment of the sample. For each group of measurements of five samples, the mean value was taken as the final data point, and the error bars were defined as the magnitude of the observed sample standard deviation [11].

2.4. DTA measurements

In additional to the above calorimetric experiments, the authors had performed DTA measurements on several selected Al–Ni alloys ($Al_{65.5}Ni_{34.5}$, $Al_{65.5}Ni_{34.5}$ and $Al_{79.45}Ni_{20.55}$, in at.%) in specific investigations, which provides some information of the phase transition temperatures and will be used for the thermodynamic refinement in Section 4.2. High-purity Al (ingot, 5 N) and Ni (wire, 4 N) were weighted and pressed into pellets with weights between 100 and 200 mg. Each pellet was heated up to a sufficient high temperature and annealed for about 15 min in DTA under Ar atmosphere. The real measurement was then carried out, normally with the heating and cooling runs at 5 K/min repeated for three times. Calibrations had been performed by measuring the melting points of pure Al (99.999%), Ag (99.995%) and Cu (99.9998%).

Three runs of DTA measurements of alloy $Al_{65.5}Ni_{34.5}$ (at.%) on heating gives very reproductive transition temperatures: 911.7 K for $L \rightarrow (Al) + Al_3Ni$, 1135.9 K for $L + Al_3Ni_2 \rightarrow Al_3Ni$, and 1408.9 K for $L + B2 \rightarrow Al_3Ni_2$. The liquidus temperature at 20.55 at.% Ni was determined to be 1265.4 K on cooling and estimated to be 1271.7 K on heating.

3. Evaluation of the heat capacity of the Al_3Ni phase

Following the recent recommendation on heat capacity models for nonmagnetic crystalline phases [12], the Debye model and the Einstein model, extended by an empirical term as given in Eqs. (1) and (2), respectively, should essentially be used for the low-temperature $C_p(T)$ evaluation and the determination of the absolute value of the standard entropy. Following that route, Unland et al. [13] worked out for GaN and InN that the more sophisticated Debye heat capacity model could provide a much better fitting to experimental data. In this work, the extended Einstein heat capacity model will be also tested and the corresponding result will be used for comparison.

$$C_p(T) = C_{Debye}(T, \theta_D) + a_D \times T + b_D \times T^2 \quad (1)$$

$$C_p(T) = C_{Einstein}(T, \theta_E) + a_E \times T + b_E \times T^2 \quad (2)$$

The empirical constants a and b are used to take care of necessary corrections to the Debye and Einstein models, including the difference $C_p - C_v$. The set of three parameters (θ_D, a_D, b_D), or alternatively (θ_E, a_E, b_E), is determined by a simultaneous least-squared fit of Eqs. (1) and (2) to the experimental data.

For the extended Debye function, the optimized parameters are:

$$\theta_D = 442.0\,\text{K}, \quad a_D = 9.030 \times 10^{-4}\,\text{J/mol K}^{-2},$$
$$b_D = 8.922 \times 10^{-6}\,\text{J/mol K}^{-3} \quad (3)$$

For the extended Einstein function, the optimized parameters are:

$$\theta_E = 310.8\,\text{K},$$
$$a_E = 1.512 \times 10^{-3}\,\text{J/mol K}^{-2}, b_E = 8.154 \times 10^{-7}\,\text{J/mol K}^{-3} \quad (4)$$

Fig. 1 shows the low-temperature capacities measured from 2 K to 323 K by relaxation measurement and the fitting curves of both the extended Debye model (Eqs. (1) and (3)) and the extended Einstein model (Eqs. (2) and (4)). As expected, the Debye model gives a much better fitting to the low-temperature $Cp(T)$ data in the whole temperature 2–323 K, than the Einstein model.

For the high-temperature (>298.15 K) heat capacity, the polynomial representation in the following form has commonly been used [14],

$$C_p(T) = a + b \cdot T + c \cdot T^{-2} + d \cdot T^2 \quad (\text{J/mol-atoms K}) \quad (5)$$

The experimental data measured by means of drop calorimetry are the heat content difference between room temperature (assumed to be 298.15 K) and each experimental temperature (T_e). The heat content can be computed by integrating $Cp(T)$ over the

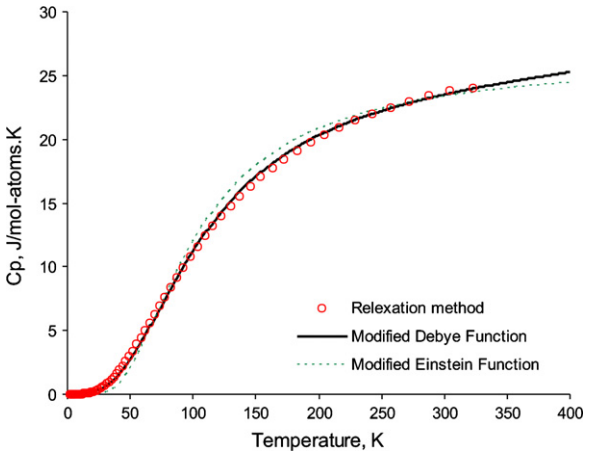

Fig. 1. Low-temperature heat capacities of the Al_3Ni phase measured by relaxation method, compared with the fitting curves by using the modified Debye model (Eqs. (1) and (3)) and the modified Einstein model (Eqs. (2) and (4)).

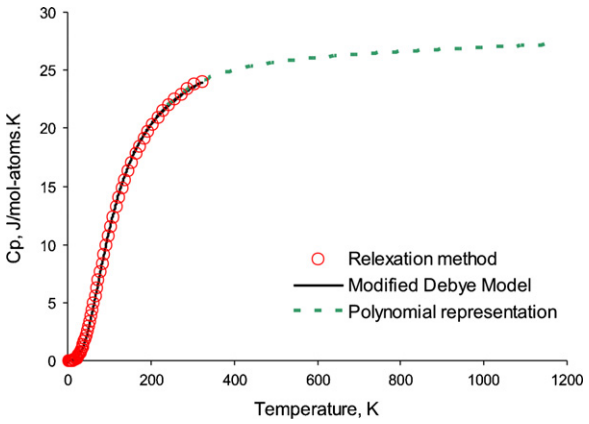

Fig. 3. Heat capacity of the Al_3Ni phase. Cycles: Data measured by relaxation method; solid line: the description by modified Debye model (Eq. (7)) for $T < 298.15$ K; dashed line: the experimentally supported description by polynomial representation (Eq. (8)) for $T > 298.15$ K.

temperature.

$$\Delta H|_{298.15}^{T_e} = \int_{298.15}^{T_e} C_p(T)\,\mathrm{d}T \quad \text{(J/mol-atoms)} \tag{6}$$

Therefore, the above equations (5) and (6) can be used in a fitting procedure of the measured heat content data to derive the parameters a to d in Eq. (5) and, thus, the expression of heat capacity. The aim of this work is to present an expression of $C_p(T)$ below 298.15 K using the extended Debye model (Eq. (1)) and above 298.15 K using the polynomial expression (Eq. (5)). Apart from the heat content data, the several data points of heat capacity above 298.15 K from the relaxation method should be used in the polynomial fitting. Actually, the data points above 250 K were used, in order to give a smooth description of $C_p(T)$ in the vicinity of 298.15 K.

Eq. (5) is a four-term polynomial and some terms may be neglected depending on the quantity and accuracy of the data. It has been found that the last term of $d{\cdot}T^2$ makes no difference to the description of $C_p(T)$ in the present fitting and thus is omitted. This agrees with common experience [14]. The resulting three-term description is sufficient to fit both the heat content data from 573 to 1073 K and the heat capacity from 250 to 323 K, as shown in Figs. 2 and 3. The third term in Eq. (5), $c{\cdot}T^{-2}$, turns out to be significant and cannot be omitted, otherwise the equation cannot describe the heat capacity from 250 to 323 K properly. Using the three terms, a to c, results in a smooth transition between high-temperature polynomial description and low-temperature Debye description. This is demonstrated in Fig. 3 where the two descriptions overlap on the graph between 250 and 323 K.

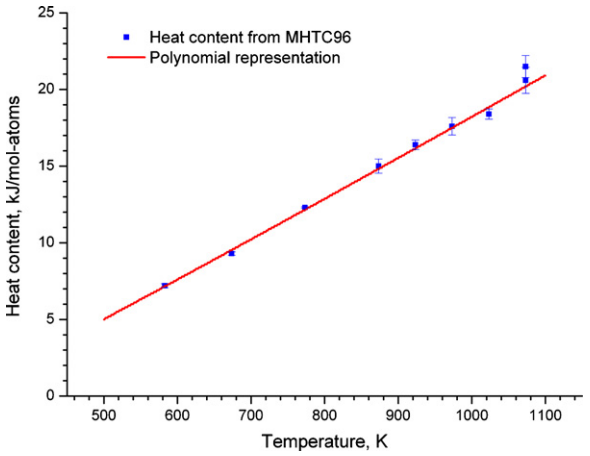

Fig. 2. Heat content of the Al_3Ni phase relative to 298.15 K. Symbols denote mean experimental data by drop calorimetry, with the error bars defined as the magnitude of the observed sample standard deviation. The solid line was calculated according to the polynomial representation (Eq. (8)).

The finally obtained description of the heat capacity of the Al_3Ni phase is given in Eqs. (7) and (8).

For $0\,\mathrm{K} < T < 298.15\,\mathrm{K}$,

$$C_p(T) = C_{Debye}(T, \theta_D) + 9.030 \times 10^{-4} T + 8.922 \times 10^{-6} T^2 \quad \text{(J/mol-atoms K)} \tag{7a}$$

$$C_{Debye}(T, \theta_D) = 9R\left(\frac{T}{\theta_D}\right)^3 \int_0^{\theta_D/T} \frac{x^4 e^x}{(e^x - 1)^2}\,\mathrm{d}x \quad \text{(J/mol-atoms K)} \tag{7b}$$

$$\theta_D = 442.0\,\mathrm{K} \tag{7c}$$

and for $298.15\,\mathrm{K} < T$,

$$C_p(T) = 26.0745 + 1.1081 \times 10^{-3} \cdot T - 2.4949 \times 10^5 \cdot T^{-2} \quad \text{(J/mol-atoms K)} \tag{8}$$

Figs. 1–3 comprehensively show that the expression given in Eqs. (7) and (8) not only agrees well with the experimental heat capacity and heat content data, but also provides a very smooth transition between the two functions in the vicinity of 298.15 K. Although the experimental data that have been used for deriving the description are available up to only 1073 K, Eq. (8) may be reasonably extrapolated somewhat above 1073 K with an almost linear dependence on the temperature.

The standard/absolute entropy S°_{298} can be determined by numerical integration of $C_p(T)/T$ over the temperature range from 0 to 298.15 K. It was calculated to be 25.4 J/mol-atoms K according to the Debye description (Eq. (7)). For comparison, it was also tried to use the Einstein description for calculating S°_{298} and it gave a value 25.5 J/mol-atoms K. The former value derived from the Debye description was accepted for S°_{298}. The perfect agreement between the heat capacity data and the Debye description, and the slight difference in the standard entropy derived from Debye model and Einstein model imply that the uncertainty for S°_{298} might be very

small.

$$S^{\circ}_{298} = 25.4\,\text{J/mol-atoms K}) \quad (9)$$

Using the standard entropy of pure Al and Ni from the SGTE compilation by Dinsdale [15], standard molar entropy of formation for the Al_3Ni phase was calculated,

$$\Delta_f S^{\circ}_{298} = -3.3\,\text{J/mol-atoms K} \quad (10)$$

4. Revision of the thermodynamic description of the Al–Ni system

A better thermodynamic description of the Al-rich portion is strived for in this work, based on the most recent modeling of the Al–Ni system [7] and the remodeling of the B2 phase [8]. First of all, the thermodynamic description of the Al_3Ni phase can be updated by taking into account the heat capacity (Eq. (8)) and the absolute entropy (Eq. (9)), together with reported enthalpy of formation in the literature. It will be modeled by using an absolute reference state. Secondly, the previous work [8] focused on the modeling of the vacancies concentration and only adjusted the parameters of the B2 phase. As a result, the B2 liquidus does not agree well with the experimental data any more. Due to the new descriptions of B2 and the Al_3Ni phase, the description of the liquid phase must be adjusted to account for the phase equilibria. Thirdly, the Gibbs energy parameters of the Al_3Ni_2 phase also need to be adjusted, not only because the phase is equilibrated with liquid, B2 and Al_3Ni, but also in order to improve the description of its homogeneity range. Especially, the slope of the solidus essentially determines the partition coefficient and the solid composition. The description of this phase is of great importance in the Scheil calculation or the phase-field modeling for solidification investigations. Additionally, the description of the Al_3Ni_5 phase will be slightly adjusted to accord with the relevant peritectoid temperature, which was not fitted by Dupin et al. [7].

The Gibbs energy functions $G_i^{\circ,\phi}(T) = G_i^{\phi}(T) - H_i^{SER}$ for the elements i (i = Al, Ni) in the ϕ phase (ϕ = liquid, fcc, bcc), where H_i^{SER} is the molar enthalpy of the stable element reference (SER) at 298.15 K and 1 bar, are taken from the SGTE compilation by Dinsdale [15].

4.1. Description of the Al_3Ni phase

The enthalpy of formation of the Al_3Ni phase has recently been determined by Chrifi-Alaoui et al. using direct reaction calorimetry [16]. It was reported to be -43.2 ± 1.1 kJ/mol-atoms relative to fcc Al and fcc Ni at 1073 K, by adopting the heat content of pure elements from Barin and Platzki [17]. The standard enthalpy of formation at 298 K was deduced to be -41.0 ± 1.1 kJ/mol-atoms from the heat content of Al_3Ni, which was not determined in the experiment, but taken from Barin and Platzki [17]. Enthalpy of formation of the alloy Al–25 at.% Ni had also been determined by early investigators Oelsen and Middel to be −38.5 kJ/mol at 298 K [18] and by Kubaschewski to be −37.7 kJ/mol at 548 K [19]. The recent First-Principle (FP) calculations due to Wang [20] and Shi et al. [21] give values of −39.6 and −42.1 kJ/mol for $\Delta_f H^{\circ}_{298}$, respectively. The above experimental data and the calculated values are slightly scattered and the experimental value of 41.0 kJ/mol-atoms [16] appears to be a good compromise.

The Al_3Ni phase had been reported to be a stoichiometric phase and its Gibbs energy had been previously described [1–7] by a floating reference state,

$$G^{Al_3Ni}(T) = 3 \cdot G^{\circ,fcc}_{Al}(T) + G^{\circ,fcc}_{Ni}(T) + A + B \cdot T \quad (11)$$

This corresponds to the simple assumption of the Neumann–Kopp-rule and one disadvantage is that the derived heat capacity of Al_3Ni will exhibit an artificial break at 933.47 K, the melting point of pure Al. That artifact is avoided by using an absolute reference state at 298.15 K, which is possible since the heat capacity and the absolute entropy of the phase are determined in this work:

$$\begin{aligned} G^{Al_3Ni}(T) &= 3 \cdot G^{\circ,fcc}_{Al}(298) + G^{\circ,fcc}_{Ni}(298) + A + B \cdot T + C \cdot T\ln(T) \\ &\quad + D \cdot T^2 + E \cdot T^3 + F \cdot T^{-1} = A^* + B \cdot T + C \cdot T\ln(T) \\ &\quad + D \cdot T^2 + E \cdot T^3 + F \cdot T^{-1} \end{aligned} \quad (12)$$

From Eq. (12), the expression for heat capacity can be given in Eq. (13). Comparing it with Eq. (8), the four coefficients C, D, E and F can be directly determined.

$$C_p(T) = -C - 2D \cdot T - 6E \cdot T^2 - 2F \cdot T^{-2} \quad (13)$$

Essentially, the other two coefficients, A^* and B, can be evaluated from the standard enthalpy of formation ($\Delta_f H^{\circ}_{298}$) and the absolute entropy (S°_{298}). In order to fit the phase equilibria data associated with the Al_3Ni phase, however, the values of A^* and B are not evaluated directly from $\Delta_f H^{\circ}_{298}$ and S°_{298}, but optimized during thermodynamic modeling by taking into account all the thermodynamic data and the phase equilibrium data. The values obtained from our final description are $\Delta_f H^{\circ}_{298} = -40.7$ kJ/mol K and $S^{\circ}_{298} = 24.7$ J/mol K, which are in good agreement with experimental data, as seen in Table 1.

Table 1
Comparison of calculated and measured standard enthalpy of formation and absolute entropy of Al_3Ni.

Data	Values	References
$\Delta_f H^{\circ}_{298}(Al_3Ni)$, kJ/mol-atoms K	−41.0	Measured [16]
	−38.5	Measured [18]
	−37.7	Measured [19]
	−39.6	FP calculation [20]
	−42.1	Shi et al. [21]
	−48.0	Calculated [7]
	−40.7	Calculated [this work]
$S^{\circ}_{298}(Al_3Ni)$, J/mol-atoms K	+25.4	Measured [this work]
	+17.2	Calculated [7]
	+24.7	Calculated [this work]

4.2. Parameter optimization of liquid, Al_3Ni_2 and Al_3Ni_5

In the present modeling, only the parameters of liquid, Al_3Ni_2 and Al_3Ni_5, together with the two coefficients, A^* and B, for Al_3Ni in Eq. (12) were allowed to be adjusted. The optimization was conducted using the computer-operated optimization program PARROT [22]. The liquid phase was treated as a substitutional solution and modeled by the Redlich–Kister equation [23]. Following the work of Dupin et al. [5,7], the Al_3Ni_2 phase was modeled using the sub-lattice model $\mathbf{Al}_3(Al,\mathbf{Ni})_2(Ni,\mathbf{Va})$. Bold font indicates the main species in each sublattice.

The experimental data on invariant equilibria had been detailedly assessed by Du and Clavaguera [3]. The best fitted data [24–28] by Du and Clavaguera [3] are identical to those exclusively selected by Huang and Chang in their modeling [4,29]. Therefore, the same selection of the invariant equilibria [24–28] is generally followed in this modeling but incorporated with the presently measured transition temperatures of the two Al-rich peritectic equilibria, as given in Table 2. The phase diagram data associated with liquid, Al_3Ni_2 and Al_3Ni reported by Refs. [24–27,30–32] were also used in the modeling, as listed in Table 3.

The enthalpies of mixing of liquid had been measured at 1923 K by Sandakov et al. [33], at 1773 K by Gizenko et al. [34], at 1800 K by Sudavtsova et al. [35], and at 1700 K by Stolz et al. [36]. No obvious temperature dependence can be observed in the plot of these data

Table 2
Calculated invariant equilibria according to this work, compared with those due to Dupin et al. [7], along with the accepted experimental data.

T (K)	Composition (at.% Ni)			Reaction, reference
	L	(Ni)	$L1_2$	$L+(Ni) = L1_2$
1645	75.5	78.5	76.2	Measured [24]
1642.6	75.5	78.7	76.0	Calculated [7]
1643.0	75.8	78.7	76.0	Calculated [this work]

T (K)	Composition (at.% Ni)			Reaction, reference
	L	B2	$L1_2$	$L = B2 + L1_2$
1642	75.2	71.0	76.0	Measured [24]
1641.8	74.7	71.0	75.2	Calculated [7]
1642.7	75.3	71.2	78.3	Calculated [this work]

T (K)	Composition (at.% Ni)		Reaction, reference
	L	B2	$L = B2$
1915	50	50	Measured [25]
1953.0	49.6	49.6	Calculated [7]
1912.1	50.3	50.3	Calculated [this work]

T (K)	Composition (at.% Ni)			Reaction, reference
	L	B2	Al_3Ni_2	$L + B2 = Al_3Ni_2$
1406	26.8	41.8	40.3	Measured [26]
1408.9	–	–	–	Measured [this work]
1400.7	25.5	41.0	40.0	Calculated [7]
1407.2	25.2	41.5	39.4	Calculated [this work]

T (K)	Composition (at.% Ni)			Reaction, reference
	L	Al_3Ni_2	Al_3Ni	$L + Al_3Ni_2 = Al_3Ni$
1127	15.4	36.0	25	Measured [26]
1135.9	–	–	–	Measured [this work]
1123.6	17.2	35.9	25	Calculated [7]
1134.7	16.0	35.7	25	Calculated [this work]

T (K)	Composition (at.% Ni)			Reaction, reference
	L	Al_3Ni	(Al)	$L = Al_3Ni + (Al)$
913	2.7	25	?	Measured [27]
914.8	2.9	25	0.2	Calculated [7]
915.1	3.1	25	0.4	Calculated [this work]

T (K)	Composition (at.% Ni)			Reaction, reference
	B2	$L1_2$	Al_3Ni_5	$B2 + L1_2 = Al_3Ni_5$
973 ± 30	~60.5	~72.8	–	Estimated [28]
914.0	58.3	72.7	62.5	Calculated [7]
973.0	58.8	72.6	62.5	Calculated [this work]

(Fig. 5). The data of Sandakov et al. [33] cover the whole composition range and appear reliable since they can be taken as a compromise of the other sets of data.

Chrifi-Alaoui et al. [16] determined the enthalpy of formation of Al_3Ni_2 to be −57.9 kJ/mol-atoms relative to fcc Al and fcc Ni at 1073 K, or −54.5 kJ/mol-atoms relative to fcc Al and fcc Ni at 298 K, which is not much higher than that of Kubaschewski [19], −57.7 kJ/mol at 548 K. Bauche et al. [37] measured the enthalpy of dissolution of Ni and Al_3Ni_2 in Al bath, and the enthalpy of formation of Al_3Ni_2 was derived to be −75.4 kJ/mol-atoms relative to solid Ni and liquid Al at 1073 K. However, such a value, corresponding to a value of −69.1 kJ/mol-atoms relative to fcc Ni and fcc Al, is noticeably too high.

4.3. Results and discussion

Table 4 gives the currently obtained parameters for Al_3Ni, liquid, Al_3Ni_2 and Al_3Ni_5, together with the parameters of B2 that had not been published [8]. Models and parameters for the other phases accepted from Dupin et al. [7] are not duplicated here. It appears that the liquid phase in the Al–Ni system could not be well described using a simple description. To account for all the thermodynamic data and phase equilibria data relevant to liquid, Du and Clavaguera [3] used an association model. Dupin et al. [7] even used the 4th-order parameters in the R–K equation [23] and it resulted in 10 coefficients, with two b-coefficients (in J/mol K) having absolute values larger than 30. It seems that Huang and Chang [4] obtained the simplest description using five coefficients, but also with a b-coefficient larger than 30. Therefore, the current description of the liquid phase appears quite reasonable.

Fig. 4 presents the Al–Ni phase diagram calculated in this work, compared with that due to Dupin et al. [7], along with both experimental data that were utilized [24–27,30–32] in the optimization and those were not used [28,38–42]. The liquidus and solidus of B2 and Al_3Ni_2 were better fitted in this work. Especially, the congruent temperature of B2 was greatly improved. Table 2 shows that the calculated temperature of the peritectic $L + B2 = Al_3Ni_2$ (1407 K) is

Table 3
Phase diagram data used in the thermodynamic revision.

Phase diagram data	Reference
Al_3Ni liquidus	Alexander and Vaughan [26] Phillips [30] Goedecke and Ellner [32]
Al_3Ni_2 liquidus	Alexander and Vaughan [26] Goedecke and Ellner [32] This work
Al_3Ni_2 solidus $Al_3Ni + Al_3Ni_2/Al_3Ni_2$	Alexander and Vaughan [26] Alexander and Vaughan [26]
B2 liquidus	Alexander and Vaughan [26] Hilpert et al. [24] Bremer et al. [31] Cotton et al. [25] Goedecke and Ellner [32]
B2 solidus	Alexander and Vaughan [26] Hilpert et al. [24] Bremer et al. [31] Cotton et al. [25]
B2 + Al_3Ni_2 tie-lines	Alexander and Vaughan [26]
(Ni) liquidus	Hilpert et al. [24] Bremer et al. [31]
(Ni) solidus	Hilpert et al. [24] Bremer et al. [31]
(Al) liquidus Invariant equilibria	Fink and Willey [27] Hilpert et al. [24] Cotton et al. [25] Alexander and Vaughan [26] Fink and Willey [27] This work

Table 4
Phase names, models (sublattice formula) and parameters for the liquid, Al_3Ni, Al_3Ni_2, Al_3Ni_5 and B2 phases given in J/mol-formula.

Liquid: $(Al,Ni)_1$

$${}^0L^{L}_{Al,Ni} = -193,695.7 + 32.9150 \cdot T$$

$${}^1L^{L}_{Al,Ni} = +15,987.4 - 12.7921 \cdot T$$

$${}^2L^{L}_{Al,Ni} = +48,276.4 - 16.4441 \cdot T$$

Al_3Ni: $Al_{0.75}Ni_{0.25}$

$$G^{\circ,Al_3Ni}_{Al:Ni} = -49,342.7 + 151.6442 \cdot T - 26.0745 \cdot T \cdot \ln(T) - 5.5405 \times 10^{-4} \cdot T^2 + 1.2475 \times 10^5 \times T^{-1}$$

Al_3Ni_2: $Al_3(Al,\mathbf{Ni})_2(Ni,\mathbf{Va})_1$

$$G^{\circ,Al_3Ni_2}_{Al:Al:Ni} = 5 \cdot G^{\circ,bcc}_{Al} + G^{\circ,bcc}_{Ni}$$

$$G^{\circ,Al_3Ni_2}_{Al:Ni:Ni} = 3 \cdot G^{\circ,bcc}_{Al} + 3 \cdot G^{\circ,bcc}_{Ni} - 427,255.7 + 87.5918 \cdot T$$

$$G^{\circ,Al_3Ni_2}_{Al:Al:Va} = 5 \cdot G^{\circ,bcc}_{Al} + 30,000$$

$$G^{\circ,Al_3Ni_2}_{Al:Ni:Va} = 3 \cdot G^{\circ,bcc}_{Al} + 2 \cdot G^{\circ,bcc}_{Ni} - 358,691.5 + 69.9029 \cdot T$$

$$L^{Al_3Ni_2}_{Al:Al,Ni:*} = -50,691.7$$

$$L^{Al_3Ni_2}_{Al:*:Ni,Va} = -33,608.5$$

Al_3Ni_5: $Al_{0.375}Ni_{0.625}$

$$G^{\circ,Al_3Ni_5}_{Al:Ni:Ni} = 0.375 \cdot G^{\circ,fcc}_{Al} + 0.625 \cdot G^{\circ,fcc}_{Ni} - 55,507.9 + 7.1800 \cdot T$$

B2: $(Al,Ni,Va)_1(Al,Ni,Va)_1$

$$G^{\circ,B2}_{Al:Al} = G^{\circ,bcc}_{Al}$$

$$G^{\circ,B2}_{Ni:Ni} = G^{\circ,bcc}_{Ni}$$

$$G^{\circ,B2}_{Va:Va} = +120,000.0$$

$$G^{\circ,B2}_{Al:Ni} = G^{\circ,B2}_{Ni:Al} = G^{\circ,bcc}_{Al} + G^{\circ,bcc}_{Ni} - 152,331.3 + 26.2275 \cdot T$$

$$G^{\circ,B2}_{Al:Va} = G^{\circ,B2}_{Va:Al} = G^{\circ,bcc}_{Al} + 7638.9$$

$$G^{\circ,B2}_{Ni:Va} = G^{\circ,B2}_{Va:Ni} = G^{\circ,bcc}_{Ni} + 68,917.3$$

$$L^{B2}_{Al,Ni:*} = L^{B2}_{*:Al,Ni} = -52,153.3 + 11.7115 \cdot T$$

$$L^{B2}_{Al,Va:*} = L^{B2}_{*:Al,Va} = +67,628.0 + 33.7081 \cdot T$$

$$L^{B2}_{Ni,Va:*} = L^{B2}_{*:Ni,Va} = -61,329.7 + 26.5974 \cdot T$$

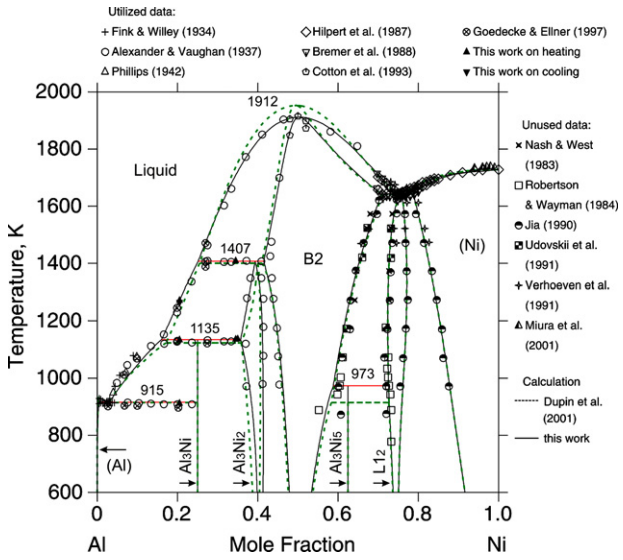

Fig. 4. Calculated Al–Ni phase diagram according to this work (solid line) and Dupin et al. [7] (dashed line), compared with experimental data that are used [24–27,30–32], this work in the modeling and those unused [28,38–42].

in much better agreement with the experimental data compared to Dupin et al. [7]. The calculated temperature for the peritectic reaction $L + Al_3Ni_2 \rightarrow Al_3Ni$ (1135 K) is noticeably higher and now in the range of experimental data, close to the present measurements (Table 2). The liquidus temperature of alloy $Al_{79.45}Ni_{20.55}$ (at.%) was measured to be 1271.7 K on heating (Section 2.4), compared to the calculated value 1273 K in this work and 1251 K using the former description [7]. The present calculation gave a very good fitting considering the steep slope of the Al_3Ni_2 liquidus. Additionally, the fitting to the temperature of the peritectoid formation of Al_3Ni_5 was greatly improved. It had been experimentally estimated to be 973 K by Robertson and Wayman [28] and the uncertainty can be expected to be less than ±30 K. The calculated value of 914 K due to Dupin et al. [7] is too low.

Fig. 5 presents the calculated enthalpy of mixing of liquid at 1923 K, with liquid Al and liquid Ni as reference states. The present description fits well to the data due to Sandakov et al. [33], with

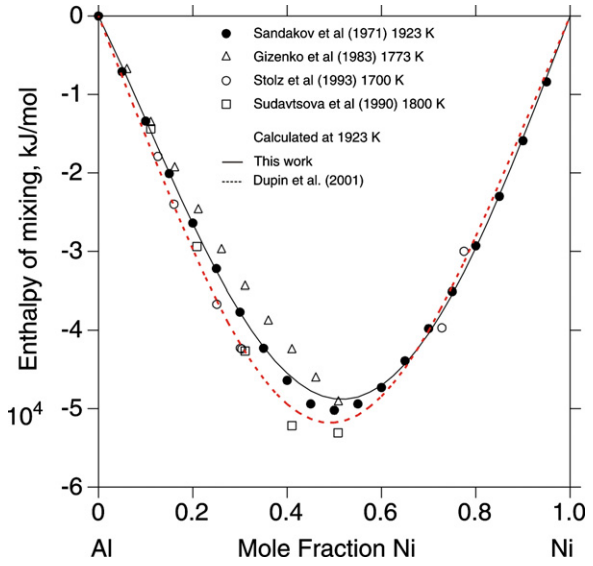

Fig. 5. Calculated enthalpy of mixing of liquid relative to liquid Al and liquid Ni at 1923 K, according to this work (solid line) and Dupin et al. [7] (dashed line), compared with experimental data [33–36].

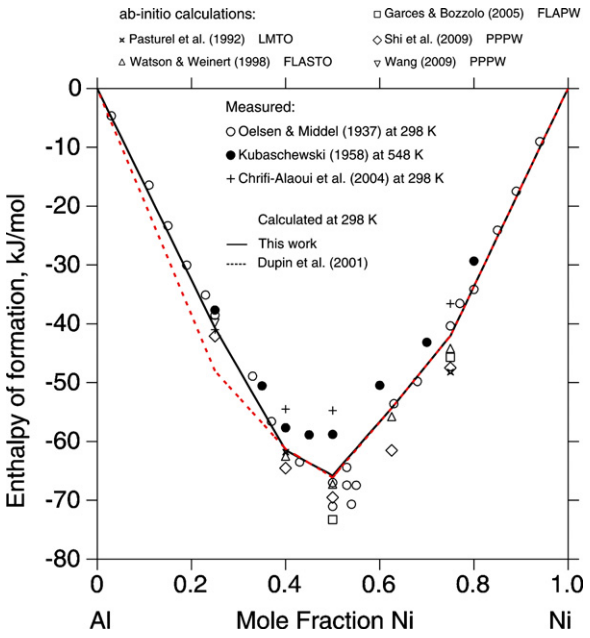

Fig. 6. Calculated enthalpy of formation relative to fcc Al and fcc Ni at 298 K, according to this work (solid line) and Dupin et al. [7] (dashed line), compared with experimental data [16,18,19], as well as the ab-initio calculations [20,21,43–45] (LMTO, linear muffin-tin orbital method; FLASTO, full-potential linearized augmented Slater-type orbital method; FLAPW, full potential linear augmented plane wave method; PPPW: pseudo-potential and plane wave method).

other data [34–36] reasonably distributed in the vicinity of the calculated curve. This calculation shows a less negative enthalpy of formation than that of Dupin et al. [7], while it is much closer to that of Huang and Chang [4].

Fig. 6 plots the calculated standard enthalpy of formation at 298 K, with experimental data, as well as the ab-initio calculation results available in literature [20,21,43–45]. The three sets of data [16,18,19] showed noticeable discrepancies in the medium composition range, so did the ab-initio results [21,43–45]. The present calculation shows a good agreement with the data of Oelsen and Middel [18] and the ab-initio calculation due to Ref. [44]. Comparing this calculation with that of Dupin et al. [7], an obvious improvement was achieved in the Al-rich range from 0 up to 40 at.% Ni because of the much better fitting to the enthalpy of formation of the Al_3Ni phase, while in the range 40–100 at.% Ni, both calculations are almost the same. It is emphasized that a significant improvement was also accomplished for the calculated value of the absolute entropy of Al_3Ni as given in Table 1. This key thermodynamic quantity was measured for the first time in the present work.

5. Conclusion

The heat capacity of the Al_3Ni phase had been measured by means of relaxation method from 2 to 323 K and drop calorimetry from 583 to 1073 K. A comprehensive representation of $C_p(T)$ was obtained by using the modified Debye model and a three-term polynomial representation below and above 298.15 K, respectively. The absolute entropy was evaluated, $S^{\circ}_{298} = 25.4$ J/mol-atoms K. The Al_3Ni phase was remodeled relative to a fixed reference state and the Gibbs energy descriptions of liquid and Al_3Ni_2 were refined by considering all the related thermodynamic data and phase equilibria. By combining these independent pieces of experimental information, the current approach ensures a consistent thermodynamic description with significant improvements on the Al-rich side of the Al–Ni system, seamlessly integrated with the well established Ni-rich B2 + $L1_2$ and $L1_2$ + (Ni) equilibria [7].

Acknowledgements

The support by the DFG (German Research Foundation) in the Priority Program SPP 1296 is gratefully acknowledged. Dr. Milan Hampl is acknowledged for instructive help in calorimetric work and Dr. Michael H.J. Jacobs is acknowledged for valuable discussions.

Appendix A. Supplementary data

Supplementary data associated with this article can be found, in the online version, at doi:10.1016/j.tca.2010.10.005.

References

[1] L. Kaufman, H. Nesor, Calphad 2 (1978) 325.
[2] I. Ansara, B. Sundman, P. Willemin, Acta Metall. 36 (1988) 977.
[3] Y. Du, N. Clavaguera, J. Alloys Compd. 237 (1996) 20.
[4] W. Huang, Y.A. Chang, Intermetallics 6 (1998) 487.
[5] I. Ansara, N. Dupin, H.L. Lukas, B. Sundman, J. Alloys Compd. 247 (1997) 20.
[6] N. Dupin, I. Ansara, Z. Metallkd. 90 (1999) 76.
[7] N. Dupin, I. Ansara, B. Sundman, Calphad 25 (2001) 279.
[8] W.A. Oates, S.L. Chen, W. Cao, F. Zhang, Y.A. Chang, L. Bencze, E. Doernberg, R. Schmid-Fetzer, Acta Mater. 56 (2008) 5255.
[9] R. Siquieri, E. Doernberg, H. Emmerich, R. Schmid-Fetzer, J. Phys. Condens. Matter 21 (2009) 464112.
[10] J. Leitner, M. Hampl, K. Ruzicka, D. Sedmidubsky, P. Svoboda, J. Vejpravova, Thermochim. Acta 450 (2006) 105.
[11] R. Willink, Accred. Qual. Assur. 14 (2009) 353.
[12] M.W. Chase, I. Ansara, A. Dinsdale, G. Eriksson, G. Grimvall, L. Hoeglund, H. Yokokawa, Calphad 19 (1995) 437.
[13] J. Unland, B. Onderka, A. Davydov, R. Schmid-Fetzer, J. Cryst. Growth 256 (2003) 33.
[14] O. Kubaschewski, C.B. Alcock, P.J. Speneer, Materials Thermochemistry, 6th ed., Pergamon, Oxford, 1993, p. 258.
[15] A.T. Dinsdale, Calphad 15 (1991) 317.
[16] F.Z. Chrifi-Alaoui, M. Nassik, K. Mahdouk, J.C. Gachon, J. Alloys Compd. 364 (2004) 121.
[17] I. Barin, G. Platzki, Thermochemical Data of Pure Substances, Parts I and II, 3rd ed., VCH, Weinheim, Germany, 1995.
[18] W. Oelsen, W. Middel, Min. Kaiser-Wilhelm-Inst. Eisenforsch. Duesseldorf 19 (1937) 1.
[19] O. Kubaschewski, Trans. Faraday Soc. 54 (1958) 814.
[20] J. Wang, private communication, 2009.
[21] D. Shi, B. Wen, R. Melnik, S. Yao, T. Li, J. Solid State Chem. 182 (2009) 2664.
[22] B. Sundman, B. Jansson, J.O. Andersson, Calphad 9 (1985) 153.
[23] O. Redlich, A. Kister, Ind. Eng. Chem. 40 (1948) 341.
[24] K. Hilpert, D. Kobertz, V. Venugopal, M. Miller, H. Gerads, F.J. Bremer, H. Nickel, Z. Naturforsch. A: Phys. Sci. 42 (1987) 1327.
[25] J.D. Cotton, R.D. Noebe, M.J. Kaufman, J. Phase Equilib. 14 (1993) 579.
[26] W.O. Alexander, N.B. Vaughan, J. Inst. Met. 61 (1937) 247.
[27] W.L. Fink, L.A. Willey, Am. Inst. Min. Metall. Eng. Inst. Met. Div. Tech. Publ. (1934) 569.
[28] I.M. Robertson, C.M. Wayman, Metallography 17 (1984) 43.
[29] W. Huang, Y.A. Chang, Intermetallics 7 (1999) 625.
[30] H.W.L. Philips, J. Inst. Met. 68 (1942) 27.
[31] F.J. Bremer, M. Beyss, E. Karthaus, A. Hellwig, T. Schober, J.M. Welter, H. Wenzl, J. Cryst. Growth 87 (1988) 185.
[32] T. Goedecke, M. Ellner, Z. Metallkd. 88 (1997) 382.
[33] V.M. Sandakov, Yu.O. Esin, P.V. Gel'd, Russ. J. Phys. Chem. 45 (1971) 1020.
[34] N.V. Gizenko, S.N. Kilesso, D.V. Ilinkov, B.I. Emlin, A.L. Zavyalov, Izv. Vyssh. Uchebn. Zaved., Tsvetn. Metall. 4 (1983) 21.
[35] V.S. Sudavtsova, A.V. Shuvalov, N.O. Sharkina, Rasplavy 4 (1990) 97.
[36] U.K. Stolz, I. Arpshofen, F. Sommer, B. Predel, J. Phase Equilib. 14 (1993) 473.
[37] K. Bouche, F. Barbier, A. Coulet, Z. Metallkd. 88 (1997) 446.
[38] P. Nash, D.R.F. West, Mater. Sci. 17 (1983) 99.
[39] C.C. Jia, PhD Thesis, Tohoku University, Japan, 1990.
[40] A.L. Udovskii, I.V. Oldakovskii, V.G. Moldavskii, V.Z. Turkevich, Dokl. Acad. Nauk SSSR 317 (1991) 161.
[41] J.D. Verhoeven, J.H. Lee, F.C. Laabs, L.L. Lones, J. Phase Equilib. 12 (1991) 15.
[42] S. Miura, H. Unno, T. Yamazaki, S. Takizawa, T. Mohri, J. Phase Equilib. 22 (2001) 457.
[43] A. Pasturel, C. Colinet, A.T. Paxton, M. van Schilfgaarde, J. Phys. Condens. Matter 4 (1992) 945.
[44] R.E. Watson, M. Weinert, Phys. Rev. B. 58 (1998) 5981.
[45] J.E. Garces, G. Bozzolo, Phys. Rev. B. 71 (2005) 134201.